DOI: https://doi.org/10.15625/0868-3166/21857

Mercury (II) sensors using Co₃O₄ films fabricated by electrochemical method

Nguyen Quoc Dung^{1,†}, Bui Dang Quang¹, Trieu Thi Anh¹, Lam Van Nang², Dang Van Thanh³, Nguyen Van Truong⁴ and Tran Dai Lam⁵

E-mail: †dungnq@tnue.edu.vn

Received 17 February 2025; Accepted for publication 10 April 2025; Published 29 May 2025

Abstract. A simple and rapid electrochemical method was developed for the synthesizing Co_3O_4 film on indium tin oxide substrate via electrochemical deposition for use as a sensing electrode to mercury (II). Morphology and structure of the Co_3O_4 film were characterized by using SEM, EDX and XRD, revealing a nanosheet structure. The synthesis conditions of the material were systematically investigated to optimize the Co_3O_4 film. The sensing properties of the fabricated electrode, evaluated by using differential pulse anodic stripping voltammetry (DP-ASV), demonstrated a linear relationship in detection range of Hg(II) ion concentration from 0.1 to 12 μ M, with a sensitivity of 14.559 μ A cm⁻² μ M⁻¹ and a detection limit of 0.06 μ M.

Keywords: cobalt oxide; mercury; electrochemical sensor; electrochemical deposition. Classification numbers: 82.47.Rs; 82.47.Wx.

1. Introduction

Heavy metals contamination in water originates not only from industrial and domestic wastewater but also from various sources, including transportation emissions, coal combustion, waste incineration, fertilizers and pesticides. Among heavy metals, mercury (Hg) is particularly

¹Faculty of Chemistry, Thai Nguyen University of Education, 20 Luong Ngoc Quyen, 24000 Thai Nguyen, Vietnam

²Department of Natural Sciences, Hoalu University, Ky Vi village, Ninh Nhat commune, Ninh Binh city, Ninh Binh Province 430000, Vietnam

³Faculty of Basic Sciences, TNU-University of Medicine and Pharmacy, 284 Luong Ngoc Quyen St., Thai Nguyen City, Thai Nguyen 25000, Vietnam

⁴Faculty of Fundamental Sciences, Thai Nguyen University of Technology, Thai Nguyen 24000, Vietnam

⁵Institute for Tropical Technology, Vietnam Academy of Science and Technology, 18 Hoang Quoc Viet, Hanoi, Vietnam

hazardous due to their persistent toxicity to humans [1]. Therefore, detecting and assessing mercury pollution levels are crucial for establishing effective mercury remediation procedures. Various methods existence for determining Hg(II) concentrations in water, such as high-performance liquid chromatography (HPLC) and atomic absorption spectroscopy (AAS). However, these methods are generally limited to stationary laboratory settings, costly, and required complex operational procedures [2]. The electrochemical sensing method offers rapid detection and high sensitivity, with the added advantage of enabling the development of portable devices. Currently, sensing materials based on metal oxides are being actively researched, particularly those with magnetic properties such as NiO [3], Co_3O_4 [4], and Fe_3O_4 [5]. These materials play a similar role in adsorption-reaction mechanisms, which can be leveraged in sensors for detecting heavy metal ions.

Cobalt oxide (Co_3O_4) is a transition metal oxide that has attracted a considerable attention in the field of electrochemical sensing, particularly with regard to the detection of heavy metal ions such as Hg(II) [6]. The suitability of Co_3O_4 for sensing applications stems from its unique physicochemical properties, including high electrochemical activity, good conductivity, and strong redox properties, which make it an ideal candidate for catalyzing electrochemical reactions. Furthermore, the stable spinel structure of Co_3O_4 provides both Co^{2+} and Co^{3+} ions on its surface, allowing for dual redox reactions that enhance the sensitivity of electrochemical sensors [7].

In addition to its excellent electrochemical properties, Co_3O_4 is also chemically stable and environmentally benign, making it suitable for real-world applications in environmental monitoring. The ability of Co_3O_4 to detect Hg(II) ions in water is of particular importance given the toxic nature of mercury, which poses serious health risks even at low concentrations.

The present study focuses on the electrochemical synthesis of Co_3O_4 as a sensing material for Hg(II) detection. The deposition of Co_3O_4 was accomplished through the utilization of electrochemical deposition, which facilitated its direct deposition on indium tin oxide (ITO) substrate. This Co_3O_4/ITO substrate functioned as the working electrode in electrochemical sensor. This method offers an advantage of precise control over the thickness and morphology of the Co_3O_4 layer, which can be tuned to optimize the sensitivity and selectivity to Hg(II) ions.

2. Experiment

2.1. Chemical and apparatus

Cobalt nitrate hexahydrate $(Co(NO_3)_2 \cdot 6H_2O)$ and lead(II) nitrate $(Hg(NO_3)_2)$ were procured from Merck. Sodium acetate anhydrous (CH_3COON_a) and acetic acid (CH_3COOH) were obtained from Xilong, China. Double-distilled water was used in the preparation of all solutions for the study. The ITO $(In_2O_3:SnO_2)$ substrate, procured from BiO Intech, China, was cut into pieces in dimension of 0.5×1.5 cm. The acetate buffer solution was prepared using sodium acetate anhydrous and acetic acid.

The study was conducted using an Autolab 302N electrochemical workstation, employing a three-electrodes setup. In this configuration, a platinum sheet served as the counter electrode, an Ag/AgCl (KCl 0.3 M) electrode functioned as the reference electrode, and the remaining electrode under investigation acted as the working electrode.

2.2. Fabrication of materials

The material was synthesized using the electrochemical deposition method in a three-electrode system, where the ITO substrate served as the working electrode. The electrochemical deposition of the material on the ITO substrate was carried out at an appropriate potential using the chronoamperometric technique, as shown in Fig. 1.

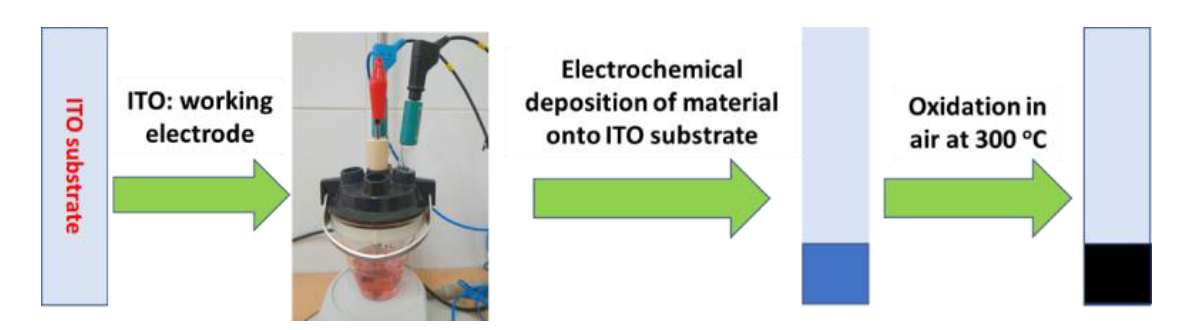


Fig. 1. Scheme of fabrication of Co₃O₄/ITO electrode.

2.3. Characterization of properties of materials

The morphology and structure of the material were characterized by scanning electron microscope (SEM: Hitachi S-4800), energy-dispersive X-ray spectroscopy (EDS: Hitachi S-4800), and X-ray diffraction (XRD: Bruker D8 Advance). The electrochemical properties of the material were investigated using a three-electrode system, where the Co₃O₄/ITO structure served as the working electrode. The concentration of Hg(II) ions in the acetate buffer solution was determined by the differential pulse anodic stripping voltammetry (DP-ASV). This technique is employed for the quantification of metal ion concentrations. This method is comprised of several stages, initiated by the electrolytic accumulation of ions onto the electrode surface at a specific potential for a predetermined duration. Subsequently, a differential pulse scan is applied in a more positive potential direction to initiate the dissolution of the deposited metal. The measurement was conducted in acetate buffer solution pH 5 that was prepared by mixing acetic acid and sodium acetate with total concentration of 0.1 M.

3. Results and discussion

3.1. CV of ITO in 0.1 M $Co(NO_3)_2$

Fig. 2 shows the cyclic voltammogram recorded for an ITO substrate used as the working electrode in a $0.1 \text{ M Co(NO}_3)_2$ solution, with the potential scanned from +0.5 V to -1.5 V at a rate of 20 mV/s. The results demonstrate a substantial increase in cathodic current density as the applied potential becomes more negative, indicating a reduction process. Within a narrower potential range, as depicted in inset of Fig. 2, the current density remains nearly zero from an initial positive potential of +0.5 V until reaching -0.620 V, at which point a noticeable increase in cathodic current density marks the onset of reduction. The formation of a blue film on the ITO substrate suggests that the deposited material is Co(OH)_2 rather than metallic cobalt, which is discussed in the following section.

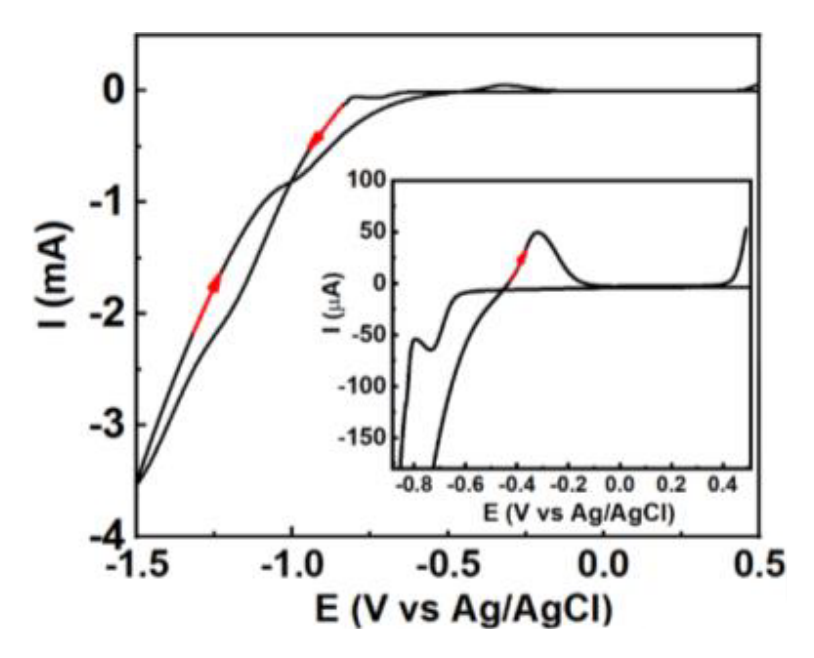


Fig. 2. CV curve of ITO in 0.1 M $Co(NO_3)_2$, under condition of potential from +0.5 to -1.5 V at scan rate of 20 mV/s.

Following analysis of the cyclic voltammetry data, we determined the optimal potentials for the electrodeposition of Co(II) onto the electrode surface. These potentials were selected to be adequate for the reduction of Co(II) ions while minimizing the potential interference from water electrolysis. Consequently, potentials of -0.8, -0.9, -1.0, and -1.1 V were chosen for subsequent studies.

3.2. Morphology and structure of materials

The electrodeposition of Co(II) onto the ITO substrate was conducted at potentials of -0.7, -0.8, -0.9, -1.0, and -1.1 V, with an electrolysis duration of 300 s. At -0.7 V, the formation of $Co(OH)_2$ on the electrode was negligible, aligning with the cyclic voltammetry data indicating that -0.7 V is the onset of the electrochemical process, where deposition is relatively slow. Attempts at a more negative potential, such as -1.2 V, resulted in the rapid detachment of the material layer from the ITO substrate. This phenomenon can be attributed to the vigorous reduction of water, which generates H_2 gas that accumulates between the deposited material and the ITO, causing the film to peel off. Gas bubble formation on the electrode surface was also observed. Therefore, $Co(OH)_2$ /ITO electrodes were fabricated at potentials of -0.8, -0.9, -1.0, and -1.1 V, with an electrolysis time of 300 s. Thereafter, the electrodes were subsequently annealed at 300 °C to produce Co_3O_4 /ITO. The surface morphology of the Co_3O_4 material on the ITO substrate is presented in Fig. 3.

The results indicate that at potentials of -0.8 V, -0.9 V, and -1.0 V, the electrode surface exhibits minimal morphological changes, with leaf-like structures present. However, at a higher potential of -1.1 V, the electrode surface becomes uneven. At higher magnification, as shown

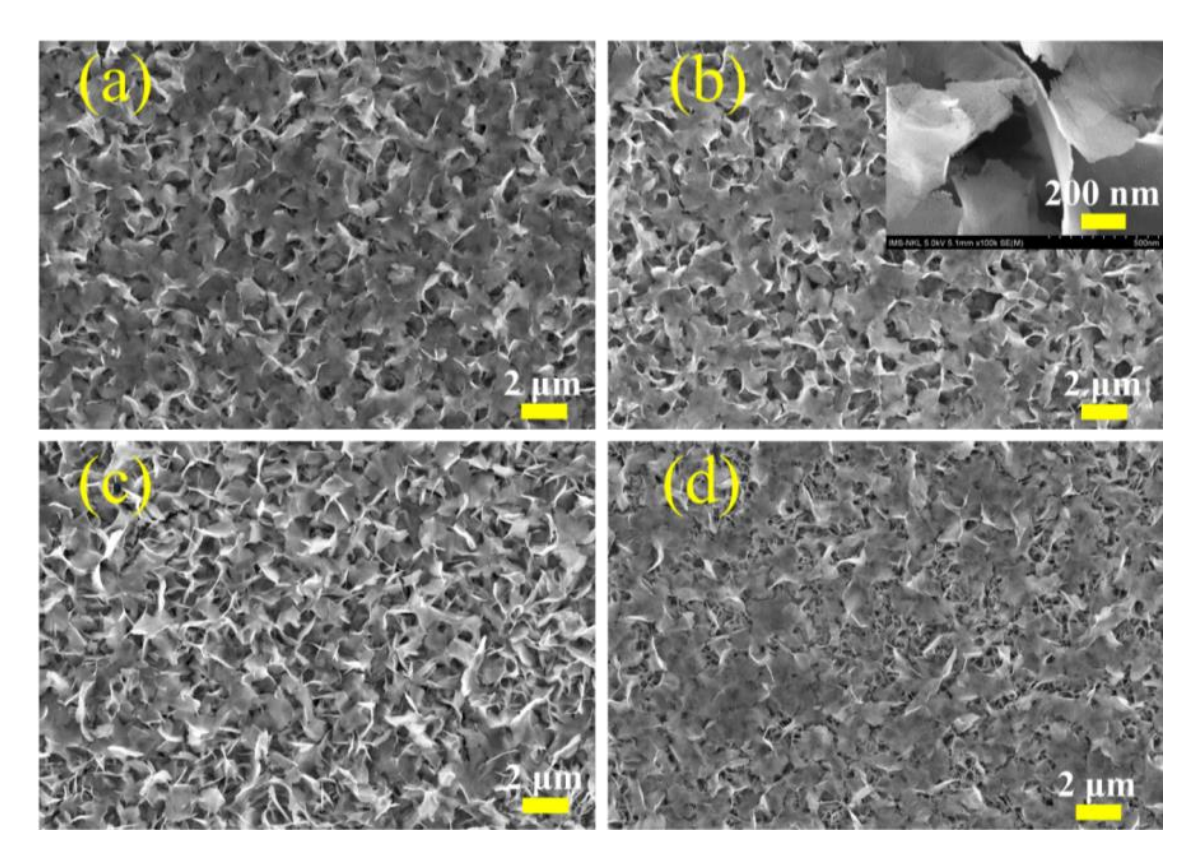


Fig. 3. SEM images of Co_3O_4 films at different electrodeposition potentials of -0.8 V (a); -0.9 V (b); -1.0 V (c); and -1.1 V (d). Inset in Fig. 3(b) showed high-magnification.

in the inset of Fig. 3(b), the SEM images reveal that the material surface is composed of sheet-like structures with two-dimensional characteristics, where the sheet width is approximately 1 μ m and thickness is less than 50 nm. This observation serves to confirm that the synthesized Co_3O_4 possesses a two-dimensional nanosheet structure. The Co_3O_4 /ITO electrode is hence designated as the CNSE (Cobalt Oxide Nanosheets Electrode). In order to ensure optimal electrolysis rate and film thickness, -0.9 V was selected as the ideal potential for electrode fabrication in subsequent experiments.

As illustrated in Fig. 4(a), the EDS spectrum of Co_3O_4 on the ITO substrate exhibits prominent peaks that correspond to O and Co elements from the Co_3O_4 material, while the remaining peaks are attributed to the ITO substrate. The structure of the material was further examined by X-ray diffraction (XRD) analysis. Fig. 4(b) presents the XRD pattern of the $Co(OH)_2$ and Co_3O_4 film on ITO. For $Co(OH)_2$ /ITO, the diffraction peaks at 33.0 and 58.8 corresponding to planes of (100) and (110). For Co_3O_4 /ITO, the diffraction peaks at 18.7, 30.1, 36.6, 59.2, and 65.1° could be indexed to (111), (220) and (311) and (440) crystal planes of Co_3O_4 phase [8]. The peaks marked with an asterisk (*) at 21.2, 30.1, 35.1, 50.4, 55.5, 60.1 represent the planes of (211), (222), (400), (440), and (622) of the ITO substrate [9] that appears in the both of $Co(OH)_2$ /ITO and Co_3O_4 /ITO.

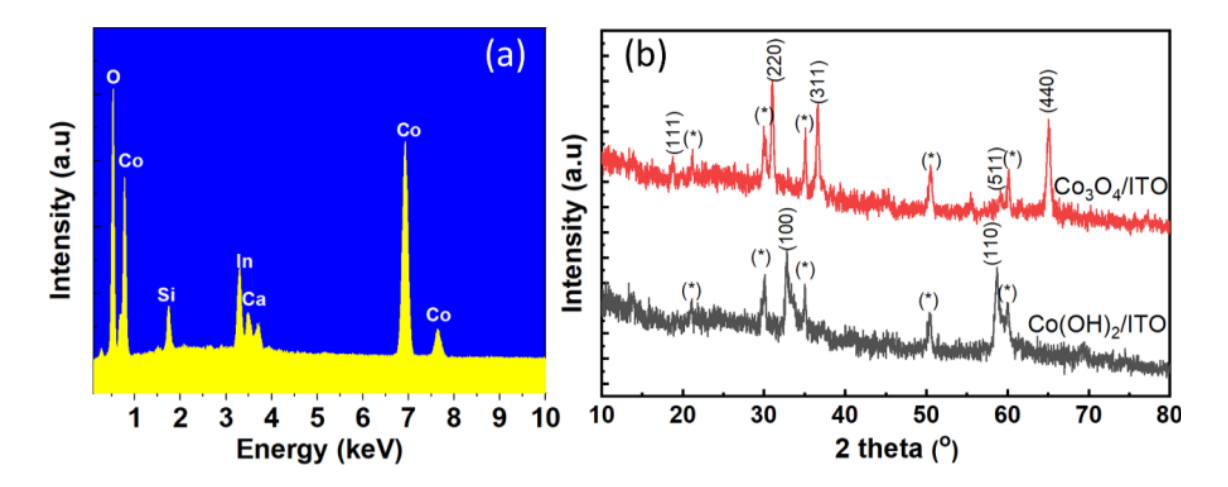


Fig. 4. (a) EDS spectrum of Co₃O₄/ITO and (b) XRD pattern of Co₃O₄/ITO.

In order to elucidate the formation of Co(OH)₂ instead of metallic Co during electrolysis, the following explanations are given.

Based on the known standard electrode potentials of the redox couples:

$$Co^{2+} + 2e \Longrightarrow Co, \quad \varepsilon_{Co^{2+}/Co}^{0} = -0.28 \text{ V}$$
 (1)

$$2H^{+} + 2e \Longrightarrow H_{2}, \quad \varepsilon_{H^{+}/H_{2}}^{0} = 0 \text{ V}. \tag{2}$$

With an electrolyte solution of 0.1 M Co(NO₃)₂, a Co(II) concentration of 0.1 M, the solution is almost neutral, semi-quantitatively calculated according to the Nernst equation: $\varepsilon_{\text{Co}^{2+}/\text{Co}} = -0.3392 \text{ V}$ and $\varepsilon_{\text{H}^+/\text{H}_2} = -0.4144 \text{ V}$.

It can be seen that, comparing the two potential values above, Co^{2+} will prioritize electrolysis first, however, the product obtained is not Co metal but $Co(OH)_2$, which means there is no reduction of Co(II). This result can be explained due to the reduction of NO_3^- ions according the following process:

$$NO_3^- + H_2O + 2e \longrightarrow NO_2^- + 2OH^-.$$
 (3)

Characterized by redox couple with electrode process:

$$NO_3^- + 2H^+ + 2e \Leftrightarrow NO_2^- + H_2O, \quad \varepsilon^0_{(NO_3^-, H^+)/NO_2^-} = 0.83 \text{ V}.$$
 (4)

In a neutral environment, according to the Nernst equation, the potential of the above redox couple is +0.42 V, a very positive value showing that NO_3^- is easily reduced during electrolysis. Therefore, the formation of $Co(OH)_2$ occurs through the following processes:

$$\begin{aligned} NO_3^- + H_2O + 2e &\longrightarrow NO_2^- + 2OH^- \\ Co^{2+} + 2OH^- &\longrightarrow Co(OH)_2. \end{aligned}$$

The formation of $Co(OH)_2$ was also mentioned in a previous study by Yu et al. [10]; however, the authors did not provide any explanations but only proposed reactions.

The appearance of a pair of peaks at -0.375 V (cathodic peak in the negative scan direction) with a cathodic current and at -0.320 V (anodic peak in the positive scan direction) with an anodic

current density is likely characteristic of the Co(OH)₃/Co(OH)₂, OH⁻ redox pair:

$$Co(OH)_3 + e \rightleftharpoons Co(OH)_2 + OH^-.$$
 (5)

On the other hand, during the negative scan, after reaching the minimum peak at -0.793 V, the current density begins to increase again, which may be attributed to an additional dehydration leading to form H_2 :

$$2H_2O + 2e \longrightarrow H_2 + 2OH^-. \tag{6}$$

In the positive scan, at a potential of 0.4 V, the anode current density suddenly increases, which may be attributed to the oxidation of water at the counter electrode (Pt) to form O₂:

$$H_2O \longrightarrow O_2 + H^+.$$
 (7)

3.3. Electrochemical properties of CNSE

3.3.1. Effect of accumulation potential

The influence of Hg accumulation during DP-ASV measurements at different accumulation potentials -0.1 to -0.9 V at 3 μ M Hg(II) was investigated, as shown in Fig. 5.

As the accumulation potential increased, the (DP-ASV) peak current density for Hg(II) exhibited a rapid increase up to -0.6 V, followed by a slower increase between -0.6 V and -0.9 V, beyond which no significant change was observed. This phenomenon can be attributed to the saturation of Hg accumulation on the electrode surface at a concentration of 3 μ M and under the investigated accumulation time conditions, commencing from -0.6 V. For subsequent studies, an accumulation potential of -0.7 V was selected to ensure optimal experimental conditions.

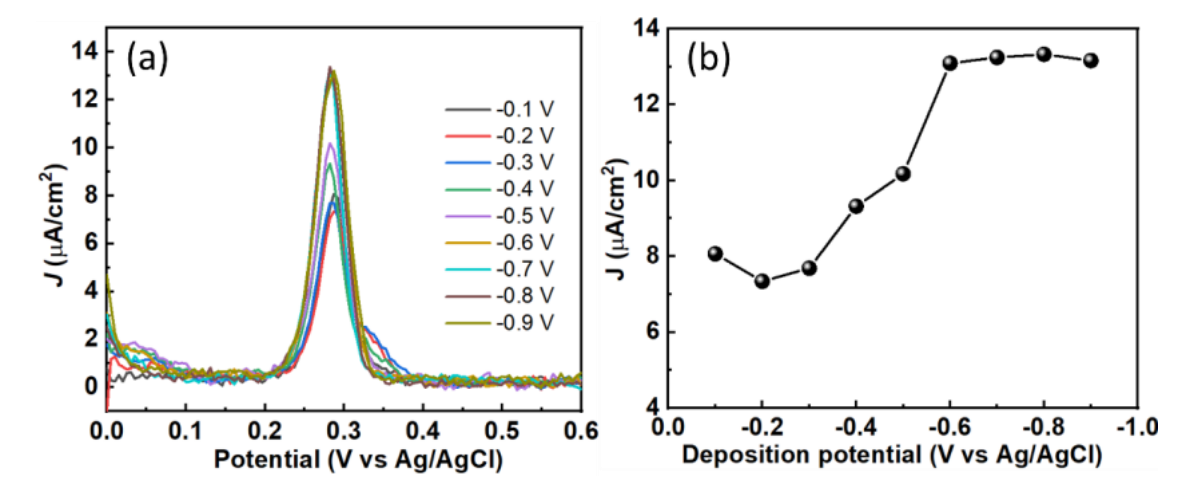


Fig. 5. (a) DP-ASV curves of CNSE for 3 μ M Hg(II) at various accumulation potentials ranging from -0.1 to -0.9 V, and (b) the dependence of DP-ASV peak current densities of Hg(II) on its concentration.

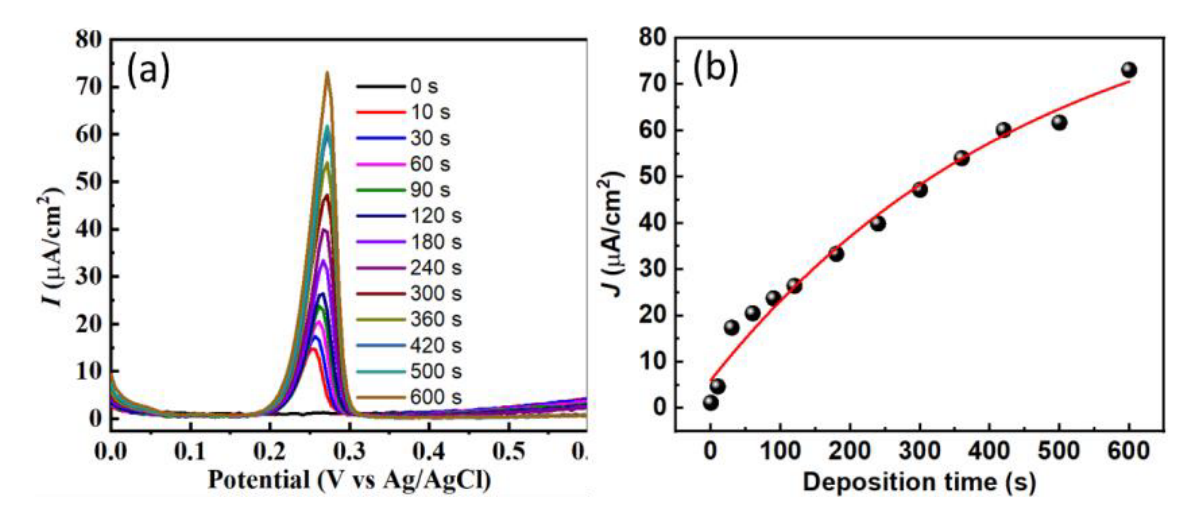


Fig. 6. (a) DP-ASV curve of CNSE as function of accumulation time and (b) Hg(II) current density peak as function of accumulation time.

3.3.2. Effect of accumulation time

The effect of accumulation time was investigated at accumulation potential -0.7 V with accumulation times from 0 s to 600 s.

Figure 6(a) illustrates that increasing the accumulation time leads to a corresponding rise in the peak height of the DP-ASV curve. This phenomenon is attributed to the extended accumulation period, which facilitates the deposition of a greater quantity of Hg on the electrode surface, thereby enhancing the peak response.

As demonstrated in Fig. 6(b), the relationship between peak current density and accumulation time reveals a rapid increase in peak height at shorter accumulation times, followed by a more gradual rise at extended times, characterized by a diminishing slope. In order to optimize the accumulation time, it is necessary to balance time efficiency with the prevention of excessive Hg accumulation, which may alter the electrode's structure and compromise its stability. It is therefore recommended that an accumulation time of 300 s be adopted for subsequent studies, as it ensures adequate Hg accumulation while minimizing the risk of electrode degradation.

3.4. Determination of Hg(II) ions in water

The DP-ASV measurements of the CNSE electrode were carried out over a range of Hg(II) concentrations ranging from 0.1 μ M to 20 μ M, as illustrated in Fig. 7. As the Hg(II) concentration increased, the peak potential shifted in a positive direction. This shift can be attributed to the greater accumulation of Hg on the electrode surface at higher concentrations, which requires a greater potential to achieve the peak current density. Additionally, the broader base of the peak indicates that a longer time is required to fully dissolve the accumulated Hg on the electrode surface.

The relationship between peak height and Hg(II) concentration is shown in Fig. 7(b). The peak height exhibited a linear increase with Hg(II) concentration up to 12 μ M, after which the slope began to decrease. The linear range was fitted with the equation $J = 14.559 \times C - 4.243$,

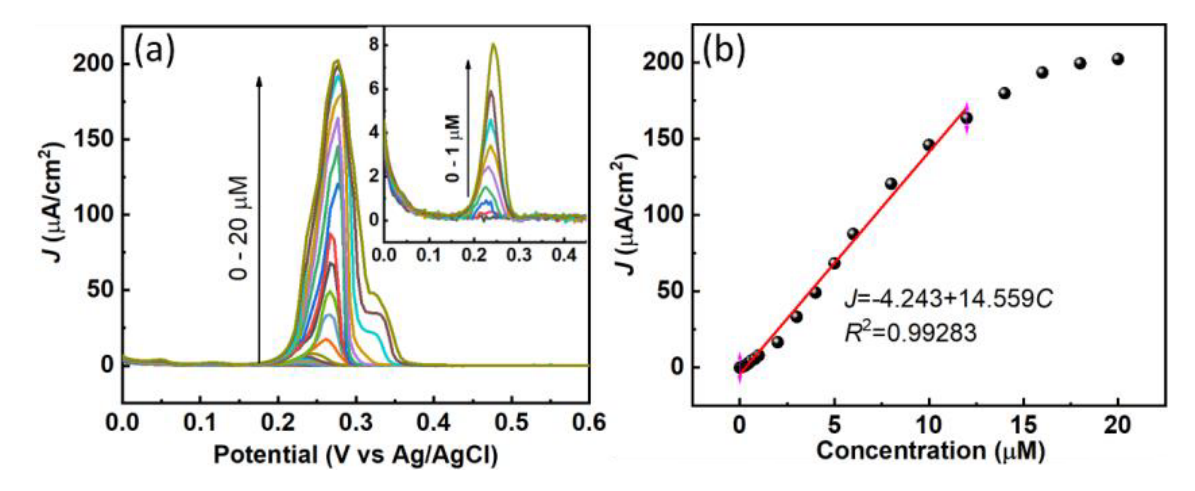


Fig. 7. (a) DP-ASV of CNSE with different concentrations of Hg(II), and (b) plot of oxidation peak current densities vs. Hg(II) concentration.

with $R^2 = 0.99283$. The sensor's sensitivity, defined as the change in current density per unit concentration of the analyte, is represented by the slope of plot of J vs. C, yielding a sensitivity of $14.559 \, \mu A \, \text{cm}^{-2} \, \mu \text{M}^{-1}$.

The detection limit (LOD) calculated according signal to nose of 3 [11] was $0.06~\mu M$. A comparison with previous studies, as shown in Table 1, demonstrates that the linear range and detection limit are within an acceptable range, indicating that the material has significant potential for further development in heavy metal ion detection sensors.

Electrode	Linear range (µM)	Sensitivity ($\mu A \text{ cm}^{-2} \mu M^{-1}$)	LOD (µM)	Reference
NCDs	0.9 - 10	_	0.15	[12]
NG/GCE	0.2 - 9	_	0.05	[13]
Steeless	0.1 - 5	93.31	0.028	[14]
C60-Chit / GCE	0.01 - 6	28.007	0.002	[15]
CNSE	0.1 - 12	14.559	0.06	This work

Table 1. Comparison of the proposed sensor's parameters with previous studies.

4. Conclusion

This study presents the successful development of an electrochemical sensor based on Co_3O_4 nanostructures for the selective detection of Hg(II) ions in solution. The synthesis of Co_3O_4 by electrochemical deposition from a $Co(NO_3)_2$ solution was shown to be both feasible and efficient. The electrolysis process facilitated the formation of $Co(OH)_2$, which subsequently underwent oxidation in an ambient conditions to yield Co_3O_4 . Notably, this work offers a novel and comprehensive explanation of $Co(OH)_2$ formation using redox potentials and the Nernst equation. The synthesized Co_3O_4 , characterized by its nanoleaf morphology, exhibited effective Hg(II) detection capabilities, with a linear response range of $0.1-12~\mu M$, a sensitivity of

14.559 $\mu A \, cm^{-2} \, \mu M^{-1}$, and a detection limit as low as 0.06 μM . This research not only underscores the potential of $Co(NO_3)_2$ as a precursor but also encourages the exploration of alternative cobalt salts for the development of advanced sensor materials.

Acknowledgement

This work was supported by Vietnam National Foundation for Science and Technology Development (NAFOSTED) under grant number 102.03-2021.125.

Conflict of interest

The authors have no conflict of interest to declare.

References

- [1] H. Teng and A. R. Altaf, Elemental mercury (Hg0) emission, hazards, and control: A brief review, J. Hazard. Mater. Adv. 5 (2022) 100049.
- [2] B. Kaur, R. Srivastava and B. Satpati, *Ultratrace detection of toxic heavy metal ions found in water bodies using hydroxyapatite supported nanocrystalline zsm-5 modified electrodes*, New J. Chem. **39** (2015) 5137.
- [3] K. Annadurai, V. Sudha, G. Murugadoss and R. Thangamuthu, *Electrochemical sensor based on hydrothermally prepared nickel oxide for the determination of 4-acetaminophen in paracetamol tablets and human blood serum samples*, J. Alloy. Compd. **852** (2021) 156911.
- [4] A. Yamuna, C.-Y. Hong, S.-M. Chen, T.-W. Chen, E. A. Alabdullkarem, M. Soylak et al., Highly selective simultaneous electrochemical detection of trace level of heavy metals in water samples based on the single-crystalline Co₃O₄ nanocubes modified electrode, J. Electroanal. Chem. 887 (2021) 115159.
- [5] A. Kulpa-Koterwa, T. Ossowski and P. Niedziałkowski, Functionalized Fe₃O₄ nanoparticles as glassy carbon electrode modifiers for heavy metal ions detection—a mini review, Materials 14 (2021) 7725.
- [6] J. Xu, Y. Zhang, X. Zhu, G. Ling and P. Zhang, Two-mode sensing strategies based on tunable cobalt metal organic framework active sites to detect Hg_2^+ , J. Hazard. Mater. 465 (2024) 133424.
- [7] Z. Zhang, Z. Liang, M. Huang, D. Shen, Z. Hu, Y. Yang et al., Design and synthesis of multilevel structured co₃o₄ double-shell dodecahedron as non-enzymatic electrochemical sensor for H₂O₂ detection, Electrochem. 92 (2024) 117003.
- [8] C.-Y. Yoo, J. Park, D. S. Yun, J. H. Yu, H. Yoon, J.-N. Kim et al., Crucial role of a nickel substrate in Co₃O₄ pseudocapacitor directly grown on nickel and its electrochemical properties, J. Alloy. Compd. **676** (2016) 407.
- [9] S. Luo, D. Yang, J. Feng and K. M. Ng, Synthesis and application of non-agglomerated ito nanocrystals via pyrolysis of indium–tin stearate without using additional organic solvents, J. Nanopart. Res. 16 (2014) 1.
- [10] L. Yu, P. Zhang, H. Dai, L. Chen, H. Ma, M. Lin et al., An electrochemical sensor based on Co₃O₄ nanosheets for lead ions determination, RSC Adv. 7 (2017) 39611.
- [11] N. Q. Dung, T. Q. Toan, P. H. Chuyen, L. V. Nang, N. V. Dang, T. N. Hien et al., Straightforward method for the electrochemical identification of dopamine in the presence of uric acid and ascorbic acid, Meas. Sci. Technol. 35 (2024) 055114.
- [12] C. Zhang, S. Wu, Y. Yu and F. Chen, *Determination of thiourea based on the reversion of fluorescence quenching of nitrogen doped carbon dots by Hg*₂⁺, Spectrochim. Acta A: Mol. Biomol. Spectrosc. **227** (2020) 117666.
- [13] X. Han, Z. Meng, H. Zhang and J. Zheng, Fullerene-based anodic stripping voltammetry for simultaneous determination of Hg(II), Cu(II), Pb(II) and Cd(II) in foodstuff, Microchim. Acta 185 (2018) 1.
- [14] S. A. Kitte, S. Li, A. Nsabimana, W. Gao, J. Lai, Z. Liu et al., Stainless steel electrode for simultaneous stripping analysis of Cd(II), Pb(II), Cu(II) and Hg(II), Talanta 191 (2019) 485.
- [15] H. Xing, J. Xu, X. Zhu, X. Duan, L. Lu, W. Wang et al., Highly sensitive simultaneous determination of cadmium (II), lead (II), copper (II), and mercury (II) ions on n-doped graphene modified electrode, J. Electroanal. Chem. 760 (2016) 52.